

# Superconductivity and Antiferromagnetic Spin Fluctuations in $\text{LaFe}(\text{As}_{1-x}\text{P}_x)(\text{O}_{1-y}\text{F}_y)$ probed by $^{31}\text{P}$ -NMR

T. Shiota<sup>a</sup>, H. Mukuda<sup>a</sup>, M. Uekubo<sup>b</sup>, F. Engetsu<sup>a</sup>, M. Yashima<sup>a</sup>, Y. Kitaoka<sup>a</sup>, K. T. Lai<sup>b</sup>, H. Usui<sup>b</sup>, K. Kuroki<sup>b</sup>, S. Miyasaka<sup>b</sup>, and S. Tajima<sup>b</sup>

<sup>a</sup>Graduate School of Engineering Science, Osaka University, Osaka 560-8531, Japan;

<sup>b</sup>Graduate School of Science, Osaka University, Osaka 560-0043, Japan

E-mail: mukuda@mp.es.osaka-u.ac.jp

**Abstract.**  $^{31}\text{P}$ -NMR study on  $\text{LaFe}(\text{As}_{1-x}\text{P}_x)(\text{O}_{0.86}\text{F}_{0.14})$  unraveled that antiferromagnetic spin fluctuations (AFMSFs) emerge significantly at  $x=0.4$  where the  $T_c$  is markedly enhanced, indicating that the AFMSFs are one of the important factors for raising  $T_c$ . From extensive comparison over wide compositions for  $0 \leq x \leq 1$  and  $0 \leq y \leq 0.14$ , we revealed that there are two different types in temperature evolution of the AFMSFs: One is enhanced particularly at low energies that evolves only at low temperatures, which mainly derives from the two orbitals of  $d_{xz/yz}$ . The other is distributed broadly at finite energies that appears up to high temperatures, which derives from three orbitals of  $d_{xy}$  and  $d_{xz/yz}$ . The highest  $T_c$  ( $=27$  K) state in the present compositions appears at  $(x,y)=(0.4, 0.1)$  where two characteristics of AFMSFs merge, suggesting the contribution of the AFMSFs over wide energies to the onset of SC. The nonmonotonic variation of  $T_c$  in  $\text{LaFe}(\text{As}_{1-x}\text{P}_x)(\text{O}_{1-y}\text{F}_y)$  is attributed to the AFMSFs from degenerated multiple-3d-orbitals on iron-pnictide superconductors.

## 1. Introduction

Superconducting (SC) transition temperature ( $T_c$ ) of a layered iron(Fe)-pnictide  $\text{LaFeAsO}_{1-y}\text{F}_y$  exhibits a broad maximum depending on  $\text{F}^-$  content, with the highest  $T_c$  of  $\sim 26$  K at  $y \sim 0.1$  [1, 2]. Further substitution of either  $\text{H}^-$  or  $\text{F}^-$  for  $\text{O}^{2-}$  uncovered the presence of the second SC dome with higher  $T_c$  than that of the first one [3, 4]. It has been known that the  $T_c$  of Fe-pnictides enhances when a  $\text{FeAs}_4$  block forms a nearly regular tetrahedral structure [5] or the height of pnictogen ( $h_{\text{Pn}}$ ) from the Fe plane is close to  $\sim 1.38$  Å [6]. However, in  $\text{LaFe}(\text{As}_{1-x}\text{P}_x)(\text{O}_{1-y}\text{F}_y)$ , the  $T_c$  values do not vary monotonously irrespective of monotonous variation of their lattice parameters with  $x$  [7, 8, 9, 10]. Previous  $^{31}\text{P}$ -NMR studies on these compounds have revealed that  $T_c$  reaches the maximum, as a result of the marked enhancement of AFM spin fluctuations (AFMSFs) at low energies [11, 12]. These AFMSFs come from the depression of re-emergent AFM2 phase in  $\text{LaFe}(\text{As}_{1-x}\text{P}_x)\text{O}$ , which exhibits at  $0.4 \leq x \leq 0.7$  of  $y=0$  that intervenes between two superconductivity (SC) phases [12, 13]. These results provide clear evidence that AFMSFs at low energies are one of the key elements for enhancing  $T_c$  in Fe-pnictide SCs even though the lattice parameters deviate from their optimum values. In this paper, we report  $^{31}\text{P}$ -NMR study on



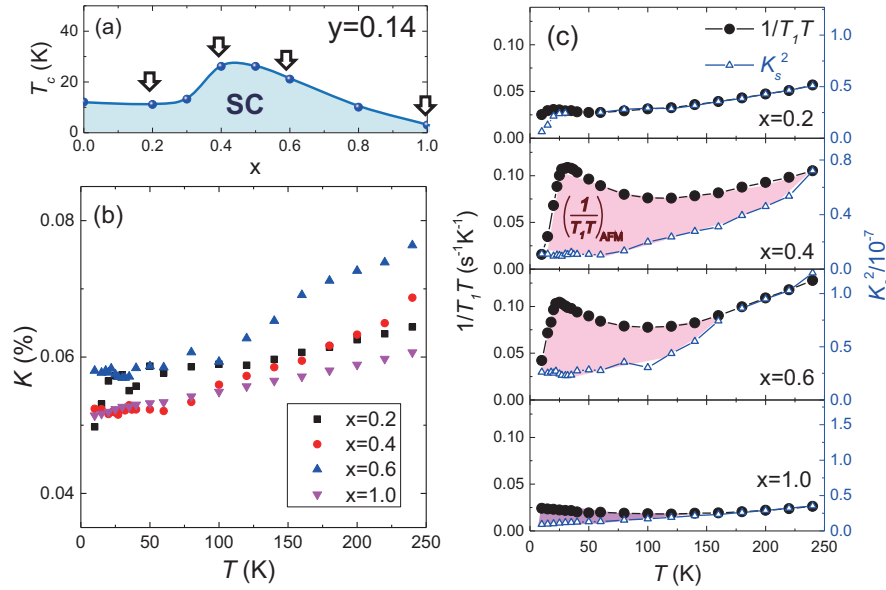


**Figure 1.** (Color online) (a)  $T_c$  vs  $x$  for  $\text{LaFe}(\text{As}_{1-x}\text{P}_x)(\text{O}_{0.86}\text{F}_{0.14})$  [10].  $T$  dependences of (b) Knight shift and (c)  $(1/T_1T)$  and  $K_s^2(T)$  for  $0.2 < x < 1.0$ . As for  $x=0.4$  and  $0.6$ ,  $(1/T_1T)$  and  $K_s(T)$  show the different behavior at low temperatures due to the development of AFMSFs with finite wave vectors.

$\text{LaFe}(\text{As}_{1-x}\text{P}_x)(\text{O}_{0.86}\text{F}_{0.14})$  to unravel the general relationship between superconductivity and the AFMSFs in the La-based 1111 series.

## 2. Experimental Procedures

Polycrystalline samples of  $\text{LaFe}(\text{As}_{1-x}\text{P}_x)(\text{O}_{0.86}\text{F}_{0.14})$  for  $0.2 \leq x \leq 1$  were synthesized by the solid-state reaction method [10, 8].  $T_c$ s are determined from an onset of SC diamagnetism as shown in Fig. 1(a)[10].  $^{31}\text{P}$ -NMR( $I=1/2$ ) measurement was performed on coarse powder samples of  $\text{LaFe}(\text{As}_{1-x}\text{P}_x)(\text{O}_{0.86}\text{F}_{0.14})$  with nominal contents  $x=0.2, 0.4, 0.6$ , and  $1.0$ , as shown by arrows in Fig. 1(a).

## 3. Results and discussion

Figures 1(b) and 1(c) show the  $T$  dependences of  $K(T)$  and  $(1/T_1T)$  for  $0.2 < x < 1.0$ , respectively. In general, the  $K$  includes the temperature( $T$ )-dependent spin shift  $K_s(T)$  and the  $T$ -independent chemical shift  $K_{\text{chem}}$ . The  $K_{\text{chem}} \sim 0.04\%$  was assumed to be the same with those of previous studies in the series[11, 12, 14, 15]. The  $T$  dependence of  $K_s^2(T)$  is shown in Fig. 1(c), together with that of  $(1/T_1T)$ . In  $x=0.2$  and  $1.0$ , the  $T$  dependence of  $(1/T_1T)$  follows that of  $K_s^2(T)$  for wide  $T$  region, which corresponds to Korringa's relation in normal metals. On the other hand, the  $(1/T_1T)$ s at  $x=0.4$  and  $0.6$  increase as  $T$  lowers, although  $K_s(T)$ s decrease. This contrasted behavior between  $(1/T_1T)$  and  $K_s(T)$  demonstrates the development of AFMSFs with finite wave vectors as  $T$  lowers. In order to deduce the development of AFMSFs following the previous studies [11, 12, 14], we assume that  $(1/T_1T)$  is decomposed as,  $(1/T_1T) = (1/T_1T)_{\text{AFM}} + (1/T_1T)_0$ , where the first term represents the contribution of AFMSFs with finite wave vectors  $Q$  presumably around  $(0, \pi)$  and  $(\pi, 0)$  and the second one does the  $q$ -independent one in proportion to  $N(E_F)^2$  i.e.  $K_s^2$ . Figure 2(a) shows a contour plot of  $(1/T_1T)_{\text{AFM}}$  for  $y=0.14$ . This plot shows that the AFMSFs develop upon cooling

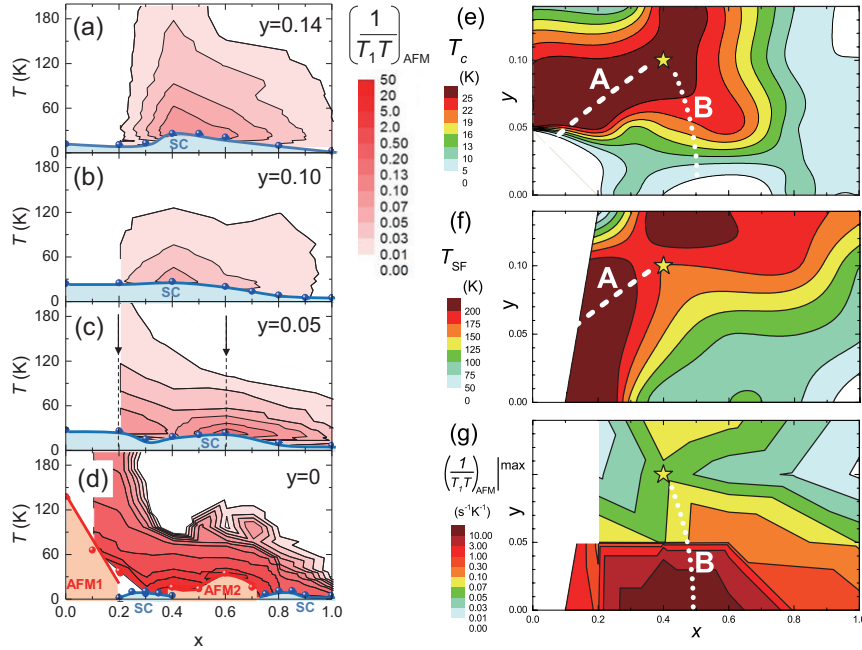


**Figure 2.** (Color online) Contour plots of  $(1/T_1T)_{\text{AFM}}$  for (a)  $y=0.14$ , along with (b)  $y=0.05$ , (c)  $0.10$ [11], and (d)  $0$ [12]. Arrows in (c) for  $y=0.05$  denote two typical types of  $T$  evolution of  $(1/T_1T)_{\text{AFM}}$ : The AFMSFs at  $x=0.2$  gradually develop upon cooling from higher  $T$ , whereas the AFMSFs at  $x=0.6$  develops rapidly only at low  $T$ , although the value of  $(1/T_1T)_{\text{AFM}}$  at low  $T$  is smaller in former case than in the latter case. Contour plots of (e)  $T_c$  [1, 2, 7, 8, 9, 10], (f)  $T_{\text{SF}}$ , and (g)  $(1/T_1T)_{\text{AFM}}^{\text{max}}$ . Here, we define  $T_{\text{SF}}$  being the temperature below which the AFMSFs start to develop, and  $(1/T_1T)_{\text{AFM}}^{\text{max}}$  being the maximum value of  $(1/T_1T)_{\text{AFM}}$ . The respective curves A and B correspond to the branches that  $T_{\text{SF}}$  and  $(1/T_1T)_{\text{AFM}}^{\text{max}}$  are relatively large. The star at  $(x, y)=(0.4, 0.1)$  denotes the highest  $T_c(=27 \text{ K})$  point.

for  $x=0.4$  and  $0.6$  exhibiting relatively high  $T_c$ , while they are drastically suppressed for  $x=0.2$  and  $1.0$  exhibiting very low  $T_c$ . The contour plots for  $y=0, 0.05$ , and  $0.1$  previously obtained are shown in Figs 2(b)-2(d), providing a clear evidence that the AFMSFs play a significant role in raising  $T_c$  in wide compositions of  $x$  and  $y$ .

However, we note that there are the two types in the  $T$ -evolution of the AFMSFs upon cooling. For example, in the two samples of  $y=0.05$  as shown by arrows in Fig. 2(c), the AFMSFs at  $x=0.6$  largely develop only at low temperatures ( $T < 100 \text{ K}$ ), whereas those at  $x=0.2$  gradually develop upon cooling from high temperatures ( $T < 250 \text{ K}$ ), although a value of  $(1/T_1T)_{\text{AFM}}$  at  $T_c$  is larger at  $x=0.6$  than at  $x=0.2$ . In order to gain further insight into these features of the AFMSFs, we define  $T_{\text{SF}}$  being the temperature below which the  $(1/T_1T)_{\text{AFM}}$  start to develop, and  $(1/T_1T)_{\text{AFM}}^{\text{max}}$  being the maximum value of  $(1/T_1T)_{\text{AFM}}$ . Thus, the  $(1/T_1T)_{\text{AFM}}^{\text{max}}$  probes a low energy limit of dynamical spin susceptibility  $\chi''(Q, \omega)$ , representing how large the spectral weight of AFMSFs are at low energies. The  $T_{\text{SF}}$  indicates the temperature that  $\chi''(Q, \omega)$  significantly starts to increase upon cooling, roughly pointing to a characteristic energy of AFMSFs. Figures 2(e), 2(f), and 2(g) show the contour plots of  $T_c$ [1, 2, 7, 8, 9, 10],  $T_{\text{SF}}$ , and  $(1/T_1T)_{\text{AFM}}^{\text{max}}$ , respectively. The curves A and B in these figures represent the relatively high  $T_c$  regions. The curve A is along the high values of  $T_{\text{SF}}$  in Fig. 2(f), in other words, roughly along the high values of the characteristic energy of AFMSFs. It indicates that the development of AFMSFs below  $T_{\text{SF}}$  is mostly responsible for raising  $T_c$ . On the one hand, the curve B are along

the large values of  $(1/T_1T)_{\text{AFM}}^{\text{max}}$ , as shown in Fig. 2(g), demonstrating that the development of the AFMSFs at low energies is also responsible for raising  $T_c$ . These two different types of  $T$ -evolution of AFMSFs are theoretically reproduced by multiple AFMSFs derived from different orbitals: The  $d_{xz/yz}$ -derived AFMSFs around the AFM2 at  $(x, y)=(0.6, 0)$  are largely enhanced at low energies, whereas the  $d_{xz/yz}+d_{xy}$  derived AFMSFs around the AFM1 at  $(x, y)=(0, 0)$  are characteristic at finite energies rather than at low energies[17, 16]. It is notable that the highest  $T_c=27$  K is denoted at  $(x, y)=(0.4, 0.1)$  by a star in Fig. 2(e) around which the curves A and B merge, suggesting the contribution of the AFMSFs over wide energies to the onset of SC.

#### 4. Summary

$^{31}\text{P}$ -NMR studies in  $\text{LaFe}(\text{As}_{1-x}\text{P}_x)(\text{O}_{1-y}\text{F}_y)$  revealed that the  $T_c$  is markedly enhanced when the AFMSFs emerge significantly, indicating that the AFMSFs are one of the important factors for enhancing  $T_c$ , even though the lattice parameters deviate from their optimum values for  $\text{FePn}_4$  regular tetrahedron. Systematic comparison of the NMR results over a series of  $\text{LaFe}(\text{As}_{1-x}\text{P}_x)(\text{O}_{1-y}\text{F}_y)$  ( $0 \leq x \leq 1$  and  $0 \leq y \leq 0.14$ ) has unraveled that there are two types in the  $T$ -evolution of the AFMSF: One is the AFMSFs that develops rapidly only at low temperature and reach the relatively high value of  $(1/T_1T)_{\text{AFM}}$  at  $T_c$ , by contrast, the other is the AFMSFs that develops gradually from high temperature upon cooling whereas the maximum value of  $(1/T_1T)_{\text{AFM}}$  is lower than that for the former. According to the theory, the former arises from the collapse of AFM2 order at  $(x,y)=(0.6, 0)$ , which derives from the good nesting of Fermi surfaces dominated mostly by  $d_{xz,yz}$  orbitals[17, 16], by contrast, the latter arises from the AFM1 order that appears at  $(x,y)=(0, 0)$ . The non-monotonic variation of  $T_c$  in  $\text{LaFe}(\text{As}_{1-x}\text{P}_x)(\text{O}_{1-y}\text{F}_y)$  is attributed to the AFMSFs derived from the multiple-orbital nature inherent to Fe-pnictide SCs.

#### References

- [1] Y. Kamihara *et al.*, J. Am. Chem. Soc. **130**, 3296 (2008).
- [2] H. Luetkens *et al.*, Nat. Mater. **8**, 305 (2009).
- [3] S. Iimura *et al.*, Nat. Commun. **3**, 943 (2012).
- [4] J. Yang *et al.*, Chin. Phys. Lett. **32**, 107401 (2015).
- [5] C. H. Lee *et al.*, J. Phys. Soc. Jpn. **77**, 083704 (2008).
- [6] Y. Mizuguchi *et al.*, Supercond. Sci. Technol. **23**, 054013 (2010).
- [7] S. Saijo *et al.*, Physica C **470**, S298 (2010).
- [8] K. T. Lai *et al.*, Phys. Rev. B **90**, 064504 (2014).
- [9] C. Wang *et al.*, Europhys. Lett. **86**, 47002 (2009).
- [10] M. Uekubo *et al.*, submitted.
- [11] H. Mukuda *et al.*, Phys. Rev. B **89**, 064511 (2014).
- [12] H. Mukuda *et al.*, J. Phys. Soc. Jpn. **83**, 083702 (2014).
- [13] S. Kitagawa *et al.*, J. Phys. Soc. Jpn. **83**, 023707 (2014).
- [14] M. Miyamoto *et al.*, Phys. Rev. B **92**, 125154 (2015).
- [15] T. Shiotani *et al.*, J. Phys. Soc. Jpn. **85**, 053706 (2016).
- [16] H. Arai *et al.*, Phys. Rev. B **91**, 134511 (2015).
- [17] H. Usui *et al.*, Sci. Rep. **5**, 11399 (2015).